Tetrahedron 67 (2011) 462–470

Contents lists available at ScienceDirect

Tetrahedron

journal homepage: www.elsevier.com/locate/tet

Enantioselective liquid–liquid extraction of (*R*,*S*)-phenylglycinol using a bisnaphthyl phosphoric acid derivative as chiral extractant

Boelo Schuur [a,d,†], Bastiaan J.V. Verkuijl [b], Jeroen Bokhove [a], Adriaan J. Minnaard [b], Johannes G. de Vries [b,c,‡,*], Hero J. Heeres [a,*], Ben L. Feringa [b,*]

[a] University of Groningen, Chemical Engineering Department, Nijenborgh 4, 9747 AG Groningen, The Netherlands
[b] University of Groningen, Stratingh Institute for Chemistry, Nijenborgh 4, 9747 AG Groningen, The Netherlands
[c] DSM Innovative Synthesis B.V., PO Box 16, 6160 MD, Geleen, The Netherlands
[d] Eindhoven University of Technology, Department of Chemical Engineering and Chemistry, Den Dolech 2, 5600 MB Eindhoven, The Netherlands

ARTICLE INFO

Article history:
Received 15 July 2010
Received in revised form 27 September 2010
Accepted 1 November 2010
Available online 5 November 2010

ABSTRACT

This study demonstrates that enantioseparation by liquid–liquid extraction can be done in a continuous flow mode on both laboratory and industrial scale and is a promising technique that could become a competitive alternative for crystallization or chromatographic approaches. We studied the enantioselective liquid–liquid extraction of phenylglycinol (Pgl) using a bisnaphthyl phosphoric acid extractant. Batch experiments were performed to estimate extraction model parameters. The system was described using an extraction mechanism with homogeneous organic phase complexation. The complexation constants were very large, in the order of 10^8–10^{10} L/mol in the temperature range $279<T<303$ K. The developed model was then used to design a multistage countercurrent extraction process with Centrifugal Contactor Separator (CCS) equipment. This study demonstrates that high purity (70% ee) with a reasonable yield (36%) can be obtained for a moderately selective system ($\alpha=1.7$) with only six extraction stages. The technology is potentially applicable to a wide range of racemates.

1. Introduction

The availability of single enantiomers of chiral compounds is essential for the pharmaceutical industry.[1] Many options are available for obtaining enantiopure compounds, e.g., using natural products (the chiral pool),[2] or by asymmetric (bio)catalysis.[3] The most abundant strategy in industry is resolution of racemates.[4] Resolution can be done via crystallization of diastereomeric salts,[5,6] (dynamic) kinetic resolution,[7–10] chromatographic methods,[11–14] electrophoretic techniques,[15,16] membrane assisted methods,[17–19] inclusion crystallization and distillation,[20] and enantioselective fluid (liquid and supercritical) extraction techniques.[21–23] Although most industrial resolutions are achieved by crystallization techniques, the technology is not always applicable and the search for a resolving agent can be rather time consuming.[18] As a result, there is an ongoing search for economically attractive alternatives.

Enantioselective liquid–liquid extraction (ELLE) is a technology that is potentially attractive for chiral separation on industrial scale. It is applicable in continuous mode on all scales from microreaction scale to multiton scale industrial separation. Scaling of the technology is relatively cheap and the continuous processing mode is advantageous by elimination of batch-to-batch variations.[24] The principle of ELLE relies on an enantioselective interaction of an extractant, for which the term host is also used,[25–28] with the substrate. The principle of host-mediated phase transfer is displayed in Fig. 1. In an ideal system, the host is confined to one of the phases and the racemate is only sparingly soluble in that phase to prevent non-selective physical transport. In such a system, if the selectivity is very high, enantioseparation can be performed in a single stage. The strength of ELLE is that such a very high selectivity is not required, but with a moderate selectivity using a multistage process high purity can still be obtained.[29,30] However, development of ELLE hosts remains a main challenge for the technology to become industrially competitive. Thus far, only a limited number of studies on ELLE have been reported. Among the variety of approaches, chiral metal complexes[31–36] have been popular for several classes of substrates, as well as the use of tartaric acid derivatives.[37–43] Furthermore, cinchona alkaloid derived

* Corresponding authors. Tel.: +31 50 363 4296; fax: +31 50 363 4278 (B.L.F); tel.: +31 50 363 4484; fax: +31 50 363 4479 (H.J.H); tel.: +31 46 476 1572; fax: +31 46 476 7604 (J.G.V); e-mail addresses: b.schuur@tue.nl (B. Schuur), hans-jg.v-ries-de@dsm.com (J.G. de Vries), h.j.heeres@rug.nl (H.J. Heeres), b.l.feringa@rug.nl (B.L. Feringa).
† Tel.: +31 40 247 4716; fax: +31 40 246 3966.
‡ Tel.: +31 50 363 4296; fax: +31 50 363 4278.

0040-4020/$ – see front matter © 2010 Elsevier Ltd. All rights reserved.
doi:10.1016/j.tet.2010.11.001

extractants have shown good enantioselectivities for amino acid derivatives.[28,44–48] Building on the work on perchlorate salts of amino acids using crown ethers with a functionalized BINOL backbone by Cram and co-workers in the 1970's,[25–27] crown ether based extractants have taken a major place in ELLE history. De Mendoza and co-workers attached a guanidine moiety to a crown ether to extract tryptophan selectively,[49] while de Haan and co-workers employed Tobe's azophenolic crown ether[50,51] in biphasic ELLE systems to extract amines and amino alcohols.[30,52,53]

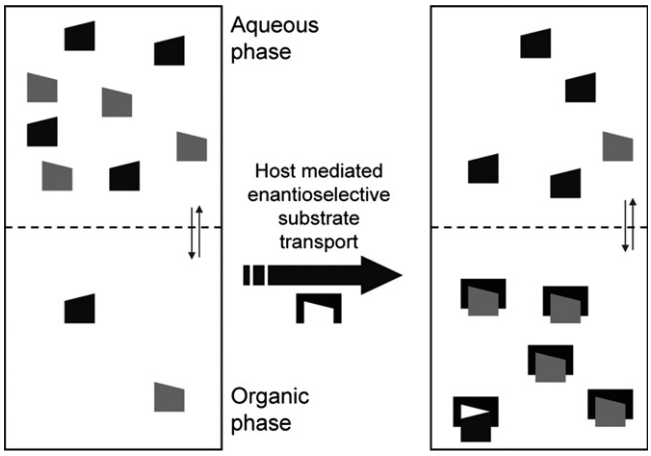

Fig. 1. Host-mediated phase transfer, the principle underlying ELLE. Symbols: grey: (*S*)-enantiomer of substrate; black: (*R*)-enantiomer of substrate; black rectangles: host or extractant. Reproduced with permission from Ref. 36, © 2009, American Chemical Society.

Instead of focusing on the crown ether part of Cram's breakthrough ELLE hosts, the BINOL backbone could also serve as scaffold for enantioselective hosts. We have recently demonstrated that $PdCl_2$(*S*)-BINAP shows a good selectivity towards a range of unprotected amino acids,[36] and have developed a BINOL based extractant for ELLE of amino alcohols and amines.[54]

In the current work, we focus on the ELLE of phenylglycinol (Pgl, see Fig. 2, left) using the extractant 3,3′-(3,5-bis(trifluoromethyl) phenyl)-2,2′-diyl hydrogenphosphate-1,1′-binaphthyl (PA1, see Fig. 2, right). This extractant was developed in our labs and showed operational selectivities of up to 2.2 towards primary amines.[54] The purely physical partitioning over the aqueous and dichloromethane (dcm) phases is examined to localize the complexation (pure interface versus homogeneous reaction). The complexation constants are determined over a temperature range from 279 to 303 K, from which the effect of the temperature on the intrinsic selectivity is determined. Also included in the studies is the temperature dependence of the protonation in the aqueous phase. The obtained parameters are used to model the extraction performance in order

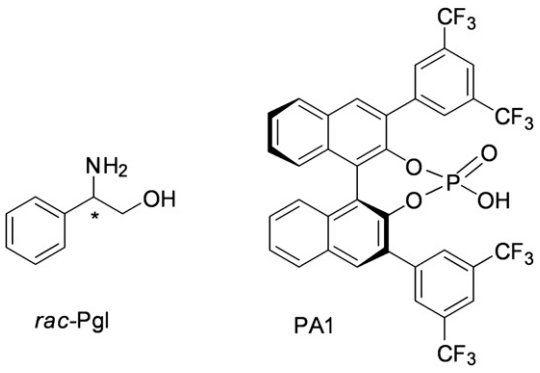

Fig. 2. Left: phenylglycinol (Pgl), right: 3,3′-(3,5-bis(trifluoromethyl)phenyl)-2,2′-diyl hydrogenphosphate-1,1′-binaphthyl.

to better understand the effect of process conditions on the ee and the yield in both single stage extractions and multistage continuous processes. Based on these insights a six stage continuous extraction process was executed to demonstrate the power of ELLE to yield high purity products based on only a limited selectivity.

The six stage continuous extraction process has been carried out using bench-scaled centrifugal contactor separators (CCS), see Fig. 3. Use of CCS-equipment is beneficial, as through the large rotational frequency of the centrifuge the mixing between the static housing and the rotating centrifuge is very intense, and the separation is very efficient because of the high centrifugal force. Because of the efficient separation, the required liquid volume is very limited and the host inventory can be greatly reduced as compared to traditional extraction column or mixer-settler processes.[28,47,48]

Fig. 3. Experimental setup of CCS devices. Six devices in line are used for the ELLE of Pgl, a seventh CCS for the back-extraction is positioned further backwards in the hood.

2. Theory

This theory section provides an overview of the terminology that is required to comprehend the results and discussion section. Most important is the selectivity. The enantioselectivity of the process is usually expressed as the operational selectivity (α_{op}).[29] In the extraction of Pgl with PA1, the (*S*)-enantiomer is the preferred extracted enantiomer and the operational selectivity is thus defined as:

$$\alpha_{op} = \frac{D_{(S)-Pgl}}{D_{(R)-Pgl}} \quad (1)$$

Here, the distributions *D* are defined as the ratios of the total concentration of all Pgl species in the organic phase over the total

concentrations in the aqueous phase.[29] For (*S*)-Pgl, the distribution is defined as:

$$D_{(S)-\mathrm{Pgl}} = \frac{[(S)-\mathrm{Pgl}]_{\mathrm{org}}^{\text{all forms}}}{[(S)-\mathrm{Pgl}]_{\mathrm{aq}}^{\text{all forms}}} \tag{2}$$

The operational selectivity (Eq. 1) is a parameter that is dependent on the extraction conditions. Even good host/substrate combinations can yield no operational selectivity if the proper conditions are not used. Therefore the operational selectivity is not a very good measure for the potential of a host/substrate combination. The intrinsic selectivity (α_{int}) is the ratio of the complexation constants, and depends only on temperature. Therefore, it is better to use the intrinsic selectivity to indicate the potential of ELLE systems. If operational conditions approach the ideal, the operational selectivity approaches the intrinsic selectivity.[52]

$$\alpha_{\mathrm{int}} = \frac{K_{cS}}{K_{cR}} \tag{3}$$

The parameter used here to define the operational performance for an extraction process is the performance factor (*PF*).[55] For the extraction system investigated, *PF* is defined as:

$$\text{(a) } PF_S = \mathrm{ee}_{\mathrm{org}} Y_{S,\mathrm{org}} \quad \text{(b) } PF_R = \mathrm{ee}_{\mathrm{aq}} Y_{R,\mathrm{aq}} \tag{4}$$

The *PF* maximum is 1.0 and occurs when full separation is obtained. Here, the ee is defined as:

$$\mathrm{ee}_k = \frac{|[(S)-\mathrm{Pgl}]_k - [(R)-\mathrm{Pgl}]_k|}{[(S)-\mathrm{Pgl}]_k + [(R)-\mathrm{Pgl}]_k} \quad (k = \mathrm{aq}, \mathrm{org}) \tag{5}$$

The yields (*Y*) are defined as the fraction of the enantiomer in the feed that ends up in the desired phase. Since the (*S*)-enantiomer is the preferred enantiomer in extraction, the yield of the (*S*)-enantiomer is considered for the organic phase and the yield for the (*R*)-enantiomer is considered for the aqueous phase:

$$\text{(a) } Y_{S,\mathrm{org}} = \frac{V_{\mathrm{org}}[(S)-\mathrm{Pgl}]_{\mathrm{org}}^{\text{all forms}}}{V_{\mathrm{aq}}[(S)-\mathrm{Pgl}]_{\mathrm{aq,init}}^{\text{all forms}}}$$

$$\text{b) } Y_{R,\mathrm{aq}} = \frac{[(R)-\mathrm{Pgl}]_{\mathrm{aq}}^{\text{all forms}}}{[(R)-\mathrm{Pgl}]_{\mathrm{aq,init}}^{\text{all forms}}} \tag{6}$$

Because in ELLE, selectivities are typically too low to obtain a high *PF* in a single stage, multistage countercurrent processing is required. In such a multistage approach, the organic and aqueous phases flow countercurrently to improve the extraction efficiency, such a countercurrent approach is displayed in Fig. 4. From Fig. 4 it follows, that in order to understand the extraction of Pgl with PA1 in a multistage approach, the required parameters are the basicity constant (K_{b}), the partition coefficient (m), and the complexation constants $K_{c,R}$ and $K_{c,S}$. The parameters are defined as:

$$K_{\mathrm{b}} = \frac{\gamma_{\mathrm{Pgl_q}H^+}\left[\mathrm{Pgl_q}H^+\right]_{\mathrm{aq}}\gamma_{OH^-}\left[OH^-\right]_{\mathrm{aq}}}{\left[\mathrm{Pgl_q}\right]_{\mathrm{aq}}} \quad (q = \mathrm{R}, \mathrm{S}) \tag{7}$$

$$m = \frac{[\mathrm{Pgl}]_{\mathrm{org}}}{[\mathrm{Pgl}]_{\mathrm{aq}}} \tag{8}$$

$$K_{\mathrm{cq}} = \frac{[(q)-\mathrm{Pgl}PA1]_{\mathrm{org}}}{[PA1]_{\mathrm{org}}[(q)-\mathrm{Pgl}]_{\mathrm{org}}} \quad (q = \mathrm{R}, \mathrm{S}) \tag{9}$$

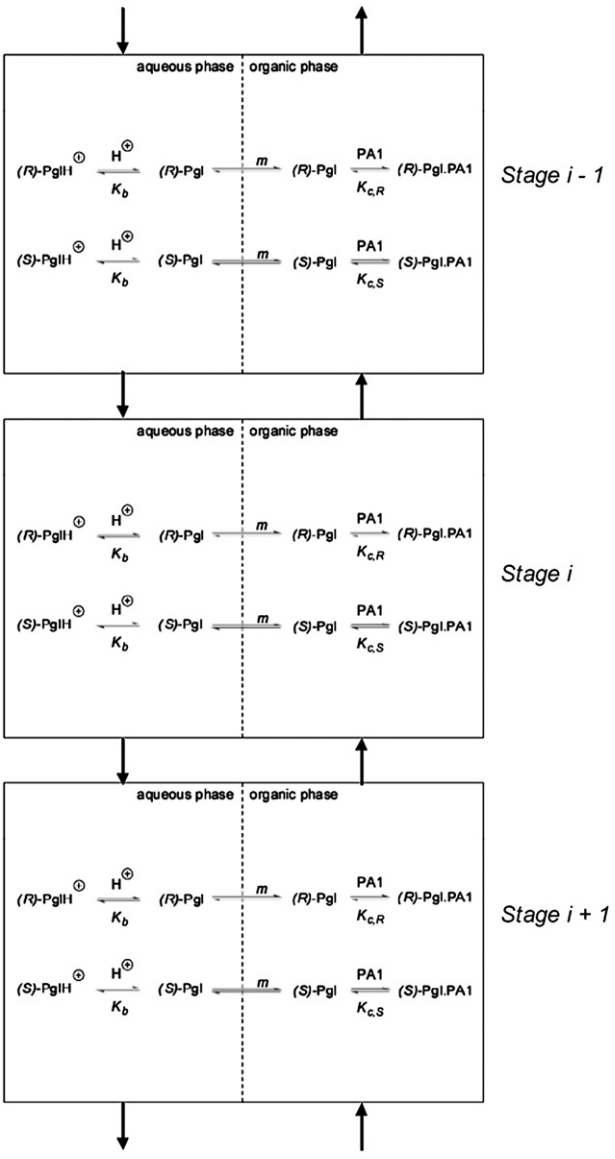

Fig. 4. Three stages in a multistage countercurrent ELLE process of Pgl using PA1 extractant.

The γ's in Eq. 7 represent the activity coefficients for ionic species in water. In case the aqueous phase ionic strength exceeds 10^{-3} mol L^{-1}, non-ideality should be taken into account.[46] The extractant PA1 was designed to be highly lipophilic, whereas Pgl partitions over the phases (vide infra), therefore the organic phase is where the complexation takes place.

3. Results and discussion

To model the extraction under equilibrium conditions, the values of the parameters K_{b}, m and the organic phase complexation constants K_{cq} need to be determined. The experimental determination of these parameters is described in the first subsection. The second subsection describes optimization of the performance factor *PF* in a single stage process to gain fundamental understanding of the effects of operating variables on the extraction performance, and in the third subsection an experimental multistage cascade process is described. The model was used to select the optimal configuration for the cascade.

3.1. Parameter estimation

3.1.1. Estimation of the temperature dependent basicity constant. Under an inert atmosphere, K_b was determined for Pgl over a temperature interval of 295–335 K by measuring the pH of aqueous solutions of Pgl. The concentration was set to $[Pgl]_{init}=3\times10^{-5}$ and 11×10^{-5} mol L^{-1}. At these concentrations, the conditions ($[Pgl]_{init}<<10^{-3}$ mol L^{-1}) can be considered ideally and the K_b may be determined from the experimentally observed $[OH^-]$ and the intake of Pgl (Eq. 10). Furthermore, Eq. 10 shows the relationship between K_b and the standard enthalpy, and entropy of reaction.[56]

$$\ln(K_b) = \ln\left(\frac{[OH^-]}{[Pgl]_{init}-[OH^-]}\right) = \frac{-\Delta H_b^\theta}{R\cdot T}+\frac{\Delta S_b^\theta}{R} \quad (10)$$

Eq. 10 was fitted to the experimental data, see Fig. 5 for the parity plot. The standard enthalpy of reaction was $\Delta H_b^\theta=-9.54\ (\pm0.09)\times10^4$ J mol^{-1} and the standard entropy of reaction was estimated at $\Delta S_b^\theta=-4.29\ (\pm0.03)\times10^2$ J mol^{-1} K^{-1}. The value of K_b was estimated to be $3.53.10^{-6}$ mol L^{-1} at room temperature, which is in accordance with the reported value in the literature.[57]

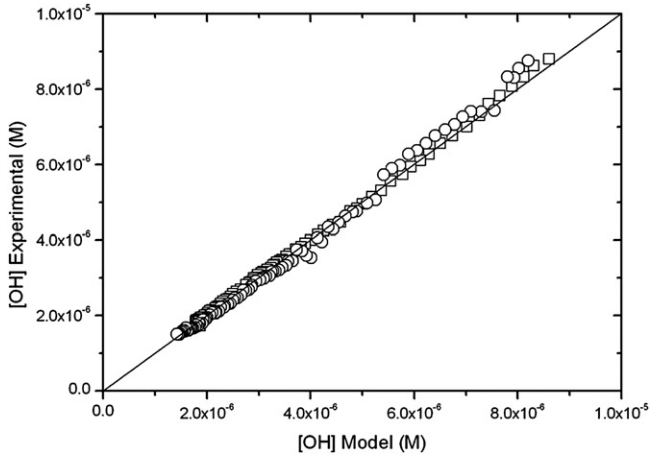

Fig. 5. Parity plot for $[OH^-]$ Symbols: □: $[PGL]_{init}=3.10^{-5}$ mol/L, ○: $[PGL]_{init}=11.10^{-5}$ mol/L.

3.1.2. Determination of the temperature dependent partitioning coefficient (m) of Pgl. The partitioning ratio (m) was determined over the temperature interval 279–303 K using Eq. 11. Eq. 11 is obtained by rewriting Eq. 8 using the mass balance for Pgl. The experimental procedure described in the Experimental section was used with $[PA1]=[PglH^+]=0.0$ mM.

$$[Pgl]_{aq} = \frac{[Pgl]_{aq,init}}{1+\phi\cdot m} \quad (11)$$

Here, ϕ is defined as the volume ratio V_{org}/V_{aq}, and $[Pgl]_{aq}$ the experimentally determined value of the two enantiomers in the aqueous phase. The value of m was fitted to the experimental data using Eq. 11 for the various temperatures. The temperature dependency of m was quantified via an empirical relation as given in Eq. 12.

$$m = a_1\cdot(T-273)^2+a_2\cdot(T-273)+a_3 \quad (12)$$

The estimated values of the coefficients a_i are given in Table 1.

Good agreement between the modeled and experimental data was confirmed, see Fig. 6.

Table 1
Estimated coefficients for Eq. 12

Coefficient	Value
a_1 [1/K²]	$-1.33(\pm0.49)\times10^{-3}$
a_2 [1/K]	$5.82\ (\pm1.63)\times10^{-2}$
a_3 [−]	$1.28\ (\pm1.24)\times10^{-1}$

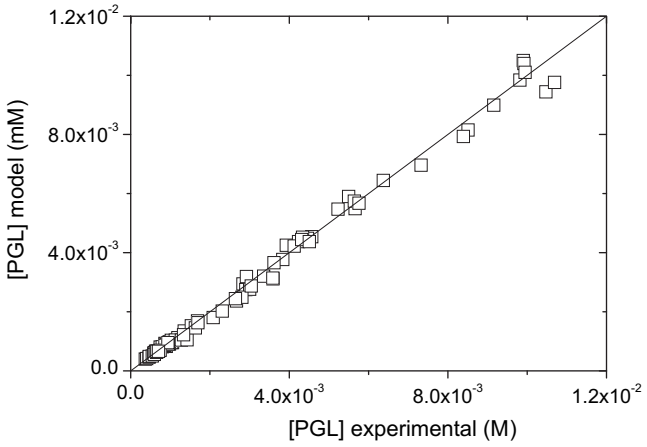

Fig. 6. Parity plot for physical partitioning parameter estimation experiments.

At T=298 K, m=0.73, which is a slightly higher value than that reported in literature[52] (m=0.6). This value of m confirms the solubility of Pgl in both the organic phase (DCM) and the aqueous phase, the requirement for use of the model with homogeneous organic phase complexation.

3.1.3. Estimation of the equilibrium constants of complexation ($K_{c,R}$ and $K_{c,S}$). Within a temperature interval of 279–303 K, reactive extraction experiments were done using enantiopure Pgl to determine the equilibrium constants of complexation $K_{c,R}$ and $K_{c,S}$. At room temperature (294 K), the values of these equilibrium constants were found to be $K_{c,R}=(8.75\pm1.12)\times10^8$ L/mol and $K_{c,R}=(1.57\pm0.17)\times10^9$ L/mol at T. The good agreement between modeled concentrations and experimental concentrations is displayed in Fig. 7.

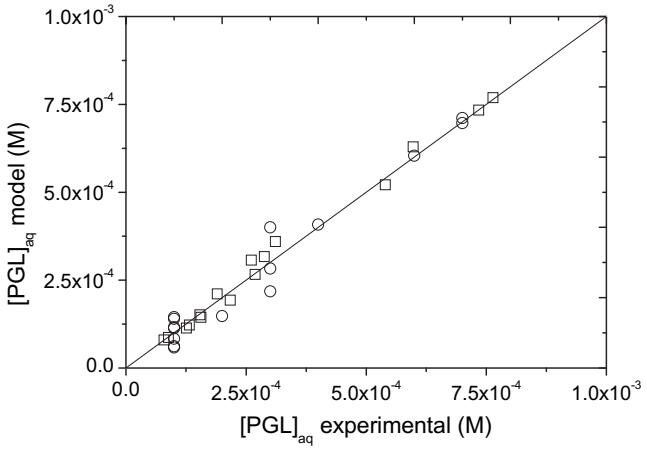

Fig. 7. Parity between extraction model and experimental data (T=294 K). Symbols: □: PGL_R, ○: PGL_S.

Similarly, at 279, 283, 288, 294, 298, and 303 K the equilibrium constants were fitted. The enthalpy and entropy of complexation, $\Delta H^\theta$and ΔS^θ, were calculated using Eq. 13 and given in Table 2.

$$\ln(K) = -\frac{\Delta H^\theta}{R\cdot T}+\frac{\Delta S^\theta}{R} \quad (13)$$

Table 2
Thermodynamic parameters of the complexation reaction of PA1 with Pgl

Entry	Substrate	ΔH^{θ} [10^5 J mol^{-1}]	ΔS^{θ} [10^2 J mol^{-1} K^{-1}]
1	(*R*)-Pgl	−1.75±0.017	−4.23±0.42
2	(*S*)-Pgl	−1.78±0.017	−4.28±0.39

The Van 't Hoff plot for the complexation is shown in Fig. 8. It can be concluded that the effect of the temperature on the intrinsic selectivity (Eq. 3) is small: the slopes for both enantiomers are essentially similar. The intrinsic selectivity shows a slight decrease on increasing temperature: from α_{int}=1.89 at 279 K to α_{int}=1.72 at 303 K, which is a behavior previously observed in ELLE.[27,52]

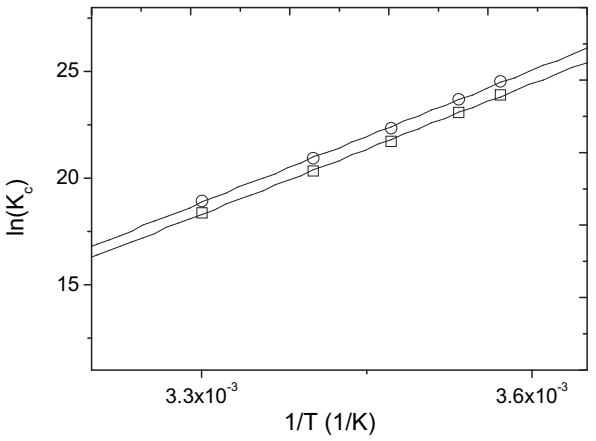

Fig. 8. Van 't Hoff plot for the complexation reaction of PA1 with Pgl. Symbols: □: (*R*)-Pgl, ○: (*S*)-Pgl.

3.1.4. Model validation. ELLE experiments of Pgl with PA1 were done over a pH interval of 1.0–8.5 to validate the model (at pH >8.5, the extractant turned out to suspend as a white solid in the aqueous phase, the extractant being responsible for the suspension was confirmed by ^{31}P NMR). During the experiments, *T*=297 K, [PA1]=0.70 mmol L^{-1}, and [Pgl]=1.0 mmol L^{-1}. As can be seen in Fig. 9, the model is valid over a broad pH range.

First, the crucial importance of the pH on the extraction performance is discussed. The effect of the pH on the ee and the yield (*Y*) is depicted in Fig. 10. Upon increasing the pH, an opposing effect is observed between the ee and the *Y*. The *Y* increases from almost 0.0 to a maximum close to 1.0 between pH=0 and 7. The ee_{org} decreases from 33% down to non-significant values. These opposing trends are the basis for the *PF* going through a maximum (0.1 at a pH of about 2). The equilibrium in the aqueous phase is accountable for this effect, as on increasing the pH, it shifts towards the neutral form of Pgl. As a result, the distribution of both enantiomers towards the organic phase is increasing. The increase of the distribution of the unwanted (*R*)-enantiomer decreases the ee_{org}, until all of the Pgl is complexed to the host. When these results are used to determine the *PF* (Fig. 11 (left), solid line) a clear maximum of *PF*=0.1 is observed at a pH around 2.

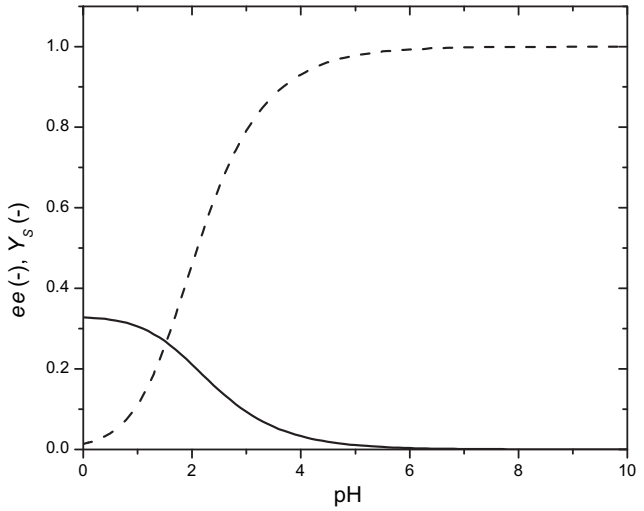

Fig. 10. The effect of pH on ee_{org} (-, solid line) and Y_S (-, dashed line). Conditions: *T*=280 K, $[Pgl]_{aq,init}$=1.0 mmol L^{-1}, $[PA1]_{org,init}$=1.0 mmol L^{-1}, ϕ=1.

To gain more insight into the effect of different host/substrate ratios, the *PF* was modeled at the same pH interval, with a decreased host concentration. While $[Pgl]_{aq,init}$ was kept at 1.0 mmol L^{-1}, $[PA1]_{org,init}$ was lowered to 0.70, 0.50 mmol L^{-1}, and 0.20 mmol L^{-1}, respectively. At 0.70 mmol L^{-1} host, after the initial optimum in the *PF*, a constant *PF* in the pH interval between 5 and 7 is observed. This is the regime in which all host is occupied. As a result, the *Y* and ee remain constant within this pH interval. At a pH above 7, the *PF* drops again as a result of the significant physical partitioning of Pgl, which results in non-

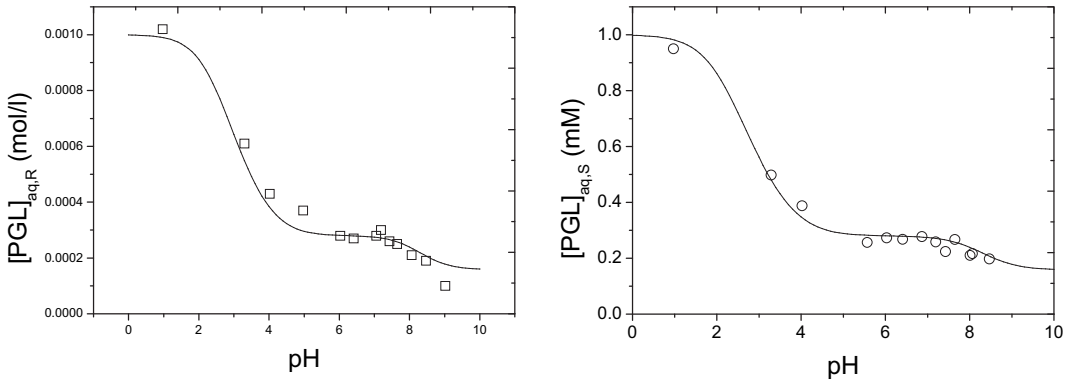

Fig. 9. Model validation over a broad pH range. (*R*)-Pgl (left), (*S*)-Pgl (right). In both figures $[PA1]_{org,init}$=0.70 mmol L^{-1} and $[Pgl]_{aq,init}$=1.0 mmol L^{-1}. Lines are model predictions, squares and circles are experimental points.

3.2. Optimization of the performance of a single equilibrium stage

The performance factor (*PF*) was defined in Eq. 4 as the product of the yield and the ee. In this section, the *PF* will be optimized to gain fundamental understanding of the effects of process conditions on the *PF*. This understanding is required for determining the right process conditions in the multistage process in next section.

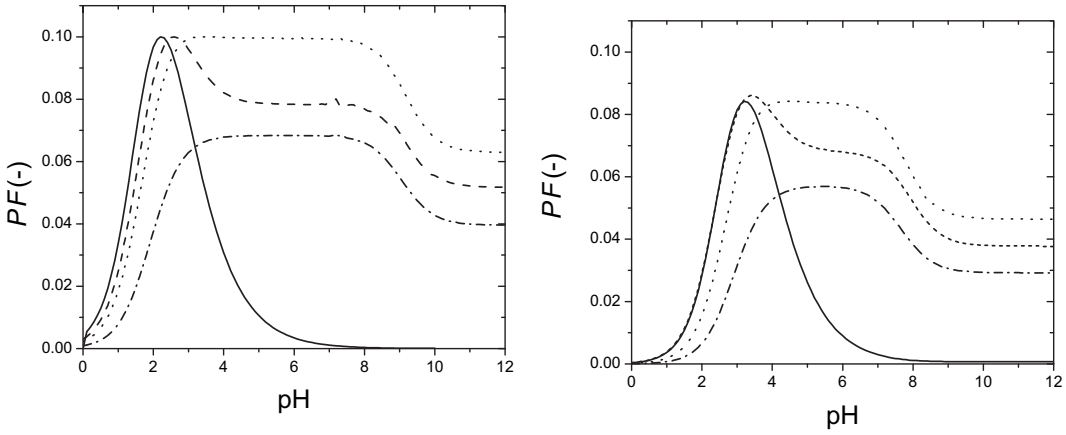

Fig. 11. *PF* at 280 K (left) and 303 K (right) at various host concentrations. $[(R),(S)\text{-Pgl}]_{aq,init}=1.0\ 10^{-3}$ mol L^{-1}, $\phi=1$. Lines: solid: $[PA1]_{org,init}=1.0$ mmol L^{-1}, dashed: $[PA1]_{org,init}=0.70$ mmol L^{-1}, dotted: $[PA1]_{org,init}=0.50$ mmol L^{-1}, dash dotted: $[PA1]_{org,init}=0.20$ mmol L^{-1}.

selective substrate transport into the organic phase. At host concentrations of 0.50 mmol L^{-1} and below, the host/guest ratio is so low that the host occupation is essentially determined by the intrinsic selectivity of the system, and therefore the plateau regime follows directly after the maximum *PF* has been reached. Finally, when the pH approaches the pK_b, a drop in *PF* is observed because of significant physical (and non-selective) partitioning. The profiles of the *PF* as a function of the pH at an increased temperature (303 K) closely resemble those of the extraction at lower temperature. However, the maximum *PF* is slightly lower (0.085) due to the decrease in intrinsic selectivity upon increasing temperature.

The results in Fig. 11 show that the *PF* is influenced by the pH, the host/guest ratio and the temperature. The maximum performance is obtained at a pH around 3 and at a low temperature. a back-extraction step (BE) in a single CCS device for recovery of the extracted (*S*)-Pgl and recycling of the host. The optimum configuration of the cascade (e.g., feed input, concentrations, flow rates) was determined by multistage equilibrium modeling of the extraction using the parameters determined in section 3.1. The mathematical model for the cascade includes the mass balances for all components (i.e., (*R*)-Pgl, (*S*)-Pgl, and PA1) and the equilibrium relations for each stage. The model predicts that 23 stages are required at room temperature to obtain both enantiomers in high ee (>99% ee). With the experimental limitation of only six CCS devices available for the cascade and one for the back-extraction unit, an arbitrary choice had to be made on which of the two enantiomers was to be obtained in high ee and reasonable yield. We selected (*S*)-Pgl to be obtained enantio-enriched in a reasonable yield using the conditions displayed in Fig. 12.

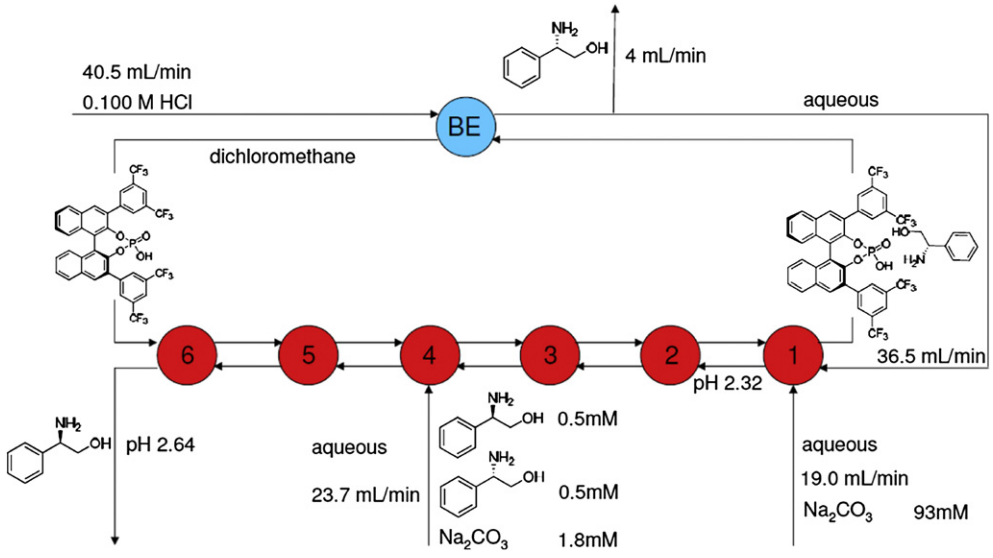

Fig. 12. Representation of the cascade with six CCS devices in series with full recovery of the host in a single back-extraction stage.

The *PF* of 0.1 is not enough to obtain the substrate with a high ee and *Y* in a single extraction step. Therefore, a fractional multistage countercurrent extraction cascade is required.

3.3. A six stage centrifugal contactor separator cascade

A cascade of six CCS devices of the type CINC V-02 (Fig. 3) with a max throughput of 1.9 L min^{-1} was applied in combination with

In an experiment aimed at obtaining enantiopure (*S*)-Pgl, 1.35 L host solution (4.3 mM) was recycled continuously through the seven CCS's with 57.1 mL min^{-1}. The feed flow ($[(R),(S)\text{-Pgl}]=1.0$ mM, $[Na_2CO_3]=1.9$ mM, pH=5.7) entered stage four at 23.8 mL min^{-1}. At stage one two separate flows entered the cascade. The reflux flow (flow rate=36.5 mL min^{-1}), containing high excess (*S*)-Pgl to increase the ee in stage one, was mixed with the wash stream (flow rate=19 mL min^{-1}). Increasing the ee in stage

one using the reflux flow affected the entire process positively, leading to a higher separation performance. The wash flow is applied to raise the pH to 2.32 and to wash the undesired (*R*)-Pgl out of the organic phase. The organic closed cycle exiting from stage one, and containing (*S*)-Pgl complexed to the host in high enantiomeric purity was then back-extracted. The host was recycled to the cascade in stage six. The (*R*),(*S*)-Pgl concentrations were monitored in both aqueous exit streams (exiting stage six and the BE stage), and all stages (1–6). The exit stream from BE is the stream with the eventual output, which contains (*S*)-Pgl with a high ee.

In the CCS cascade, the three most important parameters are the temperature, the pH in the aqueous phase, and the host concentration in the organic phase. They govern the distribution and the *PF*, and are preferentially kept stable. In the hours before starting the measurements of the experiments ($-240<t<0$ min), it became clear that (a) The temperature was stable at 295 +/−1 K. (b) The selected solvent (dcm) was evaporating at a much higher rate than we expected. Therefore, a small pump was installed pumping additional dcm into the system at a rate of about 1 mL min^{-1} (in a previous study we added solvent in small portions manually.[48]) (c) The pump responsible for the flow rate of the wash flow had to be adjusted carefully to obtain the desired pH of 2.32. The pH fluctuated between 2.63 and 1.37 before a steady operation was reached ($t=0$ min) with an actual flow slightly higher than the intended 19 mL min^{-1}. After 60 min running steady, the pump responsible for the wash flow broke down. As a result, the pH dropped below 2.32, which is visualized in the concentration profile of the exit stream from BE and shows a decrease in the concentration (see Fig. 13). This is a direct consequence of the lower pH, which lowers the distribution and keeps the Pgl confined in the aqueous phase. After solving the pump problem, the pH was restored to 2.32 and the concentration showed a steady state in the interval $120<t<180$ min.

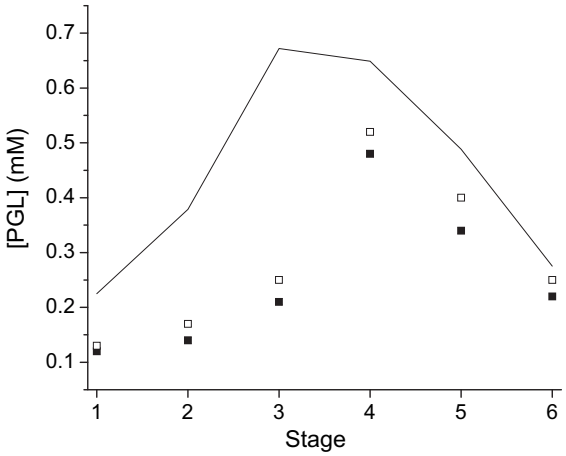

Fig. 14. Concentration profile over the cascade. Closed symbols: 147 min. Open symbols: 177 min. Line: model prediction.

147 to 177 min, the moment we had to stop the experiment. In our previous work the time taken to reach equilibrium was about 4 h.[48] It can thus be expected that the resemblance between experimental results and the model prediction are much closer if the system is allowed to reach equilibrium. In addition, the system moving back to the steady-state after the unintended pH-shock demonstrates the robustness of the system and the chemistry. Based on the steady-state yields, and the observed robustness of the chemistry (see Ref. 54), with this type of six stage cascade of CINC V-02′s, as much as 5 kg of racemate per week can be separated with corresponding results, using 380 g of host, which is not consumed, but continuously used and recycled in the process. For higher purity product, the number of stages should be increased, e.g., for the current intrinsic enantioselectivity of 1.7, some 23

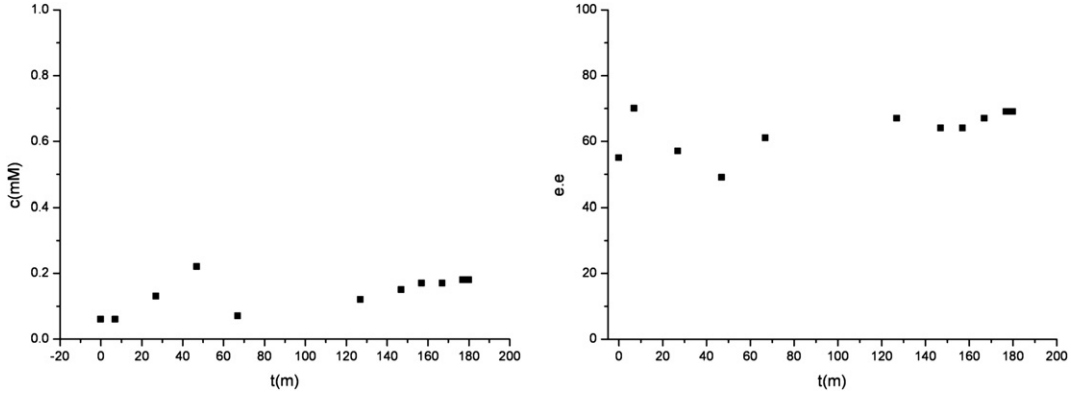

Fig. 13. Concentration (left) and ee (right) profile of the stream exiting from BE.

In the steady state interval a [Pgl]=0.18 mM (model: 21 mM) and ee=70% were found, corresponding to a yield of 36% with respect to the desired enantiomer. The agreement with the model prediction was reasonable. A clearer overview at the process is provided by plotting the concentrations throughout the stages (Fig. 14).

The concentration and profiles throughout the setup are depicted in Fig. 14. In general, it may be concluded that the trend predicted by the model is also observed experimentally. It is though clear, that although the concentration in the exiting stream from BE appears to be at steady-state (Fig. 13), the system was not yet at steady-state after the pH-shock caused by the broken pump. The concentration profile is moving towards the model line from stages are required to obtain both enantiomers in more than 99% ee. To our opinion, a 23 stage extractive enantioseparation is not excessive, but in the development of new systems, a high selectivity of >5 is desired to limit the number of stages to less than 10 for a pair of highly pure (>99% ee) single enantiomers.

4. Conclusions

We have studied the enantioselective liquid–liquid extraction (ELLE) of phenylglycinol in both batch experiments and in continuous centrifugal contactor separator (CCS) equipment using a countercurrent setup to investigate the potential of this chiral separation technology. The batch experiments were used to gain

understanding of the effects of process variables on the yield and the ee. The parameters determined with the batch experiments were used for experimental design of the multistage continuous process. (*S*)-Phenylglycinol was thus extracted preferentially from the racemic aqueous feed into a bisnaphthyl phosphoric acid extractant containing dichloromethane phase, followed by a back-extraction to recycle the extractant. The extracted (*S*)-phenylglycinol was obtained in an ee as high as 70% with a yield of 36% in only six extraction stages were used, while the system exhibited only a moderate selectivity of 1.7. From the current work it may be concluded that multistage continuous ELLE can be used to obtain highly enantiopure chiral compounds even with limitedly selective systems. The bench-scaled CCS equipment allows production scales of several kg/week, while also mg scaled batches may be separated continuously, allowing approval of a continuous process in an early development stage. Analogously to the chromatographic techniques but much less expensive in scale-up, by aiming at moderate selectivity it may be possible to apply single extractants for enantioseparation of a broad range of substrates to significantly reduce the costly time-to-market.

5. Experimental

5.1. Chemicals

The extractant, 3,3′-(3,5-bis(trifluoromethyl)phenyl)-2,2′-diyl hydrogen phosphate-1,1′-binaphthyl, was synthesized as described previously.[54] (*R*)-Phenylglycinol (98%) and (*S*)-phenylglycinol (98%) were obtained from Sigma–Aldrich. *rac*-Phenylglycinol and dichloromethane (dcm) were obtained from Acros. Potassium dihydrogen phosphate (*pa*), di-sodium hydrogen phosphate dodecahydrate (*pa*), glacial acetic acid, hydrogen chloride (37%), potassium chloride (*pa*), and sodium acetate trihydrate (*pa*) were obtained from Merck. All experiments were performed with double distilled water.

5.2. Experimental procedures

5.2.1. Batch experiments for localization of complexation and parameter estimation.

5.2.1.1. Physical extraction experiments. To determine the physcial partioning of Pgl, experiments were performed with dcm as organic phase and buffered (0.100 mol L^{-1} phosphate buffer, pH=10.0) aqueous Pgl-solutions to determine the temperature dependent partitioning behavior of non-dissociated Pgl. A pH of 10.0 was selected to ensure that most Pgl was in its neutral, non-dissociated form. In all experiments the total liquid volume was 15.0 mL, the volume ratio $\phi=V_{org}/V_{aq}$ was varied between 0.19 and 2.61, the temperature between 279 and 303 K, and the initial Pgl concentration between 9×10^{-4}and14×10^{-3} mol L^{-1}. The two phase systems were stirred vigorously for 12 h, after which the phases were allowed to settle. Samples were taken from the aqueous phase and analyzed by RP-HPLC equipped with a Crownpak(+) column. The organic phase concentrations were calculated using the overall mass balance.

5.2.1.2. Estimation of the basicity constant (K_b) of Pgl. To determine the temperature dependent basicity constant (K_b) of Pgl, the pH of diluted Pgl solutions was measured while heating the well stirred solutions at a rate of 1 K min^{-1}. Two experiments were performed with different Pgl concentrations (3×10^{-5} mol L^{-1} and 11×10^{-5} mol L^{-1}) in the temperature range of $295<T<335$ K. The experiments were conducted under an inert atmosphere.

5.2.1.3. Reactive extraction experiments. The reactive extraction experiments were performed using aqueous solutions of enantiopure (*q*)-Pgl (*q*=R or S) and solutions of PA1 in dcm at varying temperatures (279–303 K), volume ratio (V_{org}/V_{aq}=0.5–1) and initial concentrations (2.5×10^{-4}–1×10^{-3} mol L^{-1} (*q*)-Pgl and 3×10^{-4}–8×10^{-4} mol L^{-1} PA1). The pH was kept constant at 3.2 (0.100 mol L^{-1} acetate buffer). The biphasic systems were stirred vigorously for 3 h to ensure equilibrium. Samples were taken from the aqueous phase and analyzed by HPLC. The organic phase concentrations were calculated by using the overall mass balance. For model verification, experiments with enantiopure (*R*)-Pgl and (*S*)-Pgl were performed at the conditions described above, except for the pH, which was varied from 1 to 8.5 (using a 0.100 mol L^{-1} HCl/KCl buffer for pH<3, a 0.1 mol/L acetate buffer for 3<pH<5, and a 0.1 mol L^{-1} phosphate buffer for pH>5).

5.2.2. Continuous ELLE in a countercurrent six stage CCS cascade. A series of six CCS devices was set up in a cascade according to Fig. 12. An additional CCS device was used as a back-extraction unit. A 1.0 mM Pgl/1.8 mM Na_2CO_3 aqueous solution of 1.5 L was used for the feed. A 93.0 mM Na_2CO_3 aqueous solution of 1.5 L was used for the wash. A 0.100 M HCl aqueous solution of 3.0 L was used for the back extraction. A dcm solution of *V*=1.35 L, [PA1]=3.6 mM, was used as the organic phase flow. Flow rates were 23.8 mL min^{-1} for the feed, 19.0 mL min^{-1} for the wash, 40.5 mL min^{-1} for the aqueous back-extraction stream, 57.1 mL min^{-1} for the organic extract stream. From the 40.5 mL min^{-1} aqueous flow exiting the back-extraction 36.5 mL min^{-1} was refluxed, and 4.0 mL min^{-1} was collected as the product stream. The CCS devices were set at a stirring rate of 40 Hz. Samples were taken frequently after all stages and from the BE outlet and analyzed using RP-HPLC

5.3. Analytical procedures

Samples (10 μL) from the aqueous phase were analyzed using reverse phase HPLC using 0.100 mol L^{-1} perchloric acid as eluent with a flow rate of 0.5 mL/min. Before injection, the samples were filtered over a PTFE syringe filter with pore size 0.45 μm (Waters Chrom). The equipment consisted of Shimadzu CC-20AD pumps, a Crownpak CR(+) chiral column (Diacel, Japan) equipped with guard column and an SPD-M20A diode array detector. Detection was done at 204 nm UV-light. Quantitative analysis (accuracy 2%) was performed using calibration curves. The pH-measurements were performed using an Inolab pH 730 pH-meter equipped with a Sentix 81 Probe.

5.4. Modeling software and optimization

Parameter fitting was performed using a nonlinear least squares method (lsqnonlin) provided by the software package Matlab (Mathworks). Confidence intervals (95%) are reported for the parameters. The model correlation parameters used are R^2 and the mean relative error (MRE).

References and notes

1. Breuer, M.; Ditrich, K.; Habicher, T.; Hauer, B.; Kesseler, M.; Sturmer, R.; Zelinski, T. *Angew. Chem., Int. Ed.* **2004**, *43*, 788–824.
2. Sheldon, R. A. *Chirotechnology; Industrial Synthesis of Optically Active Compounds*; Marcel Dekker: New York, NY, 1993.
3. Jacobsen, E. N.; Pfaltz, A.; Yamamoto, H. *Comprehensive Asymmetric Catalysis*; Springer: Berlin, 1999.
4. Carey, J. S.; Laffan, D.; Thomson, C.; Williams, M. T. *Org. Biomol. Chem.* **2006**, *4*, 2337–2347.
5. Liu, W. In *Handbook of Chiral Chemicals*, 2nd ed.; Ager, D. J., Ed.; Taylor & Francis: Boca Raton, FL, 2006, pp 75–95.
6. Kozma, D. *CRC Handbook of Optical Resolutions via Diastereomeric Salt Formation*; CRC LLC: Boca Raton, 2002.
7. Collins, A. N.; Sheldrake, G. N.; Crosby, J. *Chirality in Industry*; John Wiley: Chichester, UK, 1992.
8. Pamies, O.; Backvall, J. E. *Chem. Rev.* **2003**, *103*, 3247–3261.

9. Patel, R. N. *Stereoselective Biocatalysis*; Marcel Dekker: New York, NY, 2000.
10. Vedejs, E.; Jure, M. *Angew. Chem., Int. Ed.* **2005**, *44*, 3974–4001.
11. Gavioli, E.; Maier, N. M.; Minguillon, C.; Lindner, W. *Anal. Chem.* **2004**, *76*, 5837–5848.
12. Seidel-Morgenstern, A.; Kessler, L. C.; Kaspereit, M. *Chem. Eng. Technol.* **2008**, *31*, 826–837.
13. Zenoni, G.; Quattrini, F.; Mazzotti, M.; Fuganti, C.; Morbidelli, M. *Flavour Fragrance J.* **2002**, *17*, 195–202.
14. Subramanian, G. *Chiral Separaration Techniques: A Practical Approach*, 3rd ed.; Wiley-VCH: Weinheim, 2007.
15. Gübitz, G.; Schmid, M. G. *Chiral Separations*; Humana: Totowa (NJ), 2004.
16. Schmitt-Kopplin, P. *Capillary Electrophoresis: Methods and Protocols*; Springer: Berlin, 2008.
17. Maximini, A.; Chmiel, H.; Holdik, H.; Maier, N. W. *J. Membr. Sci.* **2006**, *276*, 221–231.
18. Xie, R.; Chu, L. Y.; Deng, J. G. *Chem. Soc. Rev.* **2008**, *37*, 1243–1263.
19. van der Ent, E. M.; Thielen, T. P. H.; Stuart, M. A. C.; van der Padt, A.; Keurentjes, J. T. F. *Ind. Eng. Chem. Res.* **2001**, *40*, 6021–6027.
20. Toda, F. In *Enantiomer Separation; Fundamentals and Practical Methods*; Toda, F., Ed.; Kluwer Academic: Dordrecht, 2004, pp 1–47.
21. de Haan, A. B.; Simandi, B. In *Ion Exch. Solvent Extr.*; Marcus, Y., Sharma, M. M., Marinsky, J. A., Eds.; 2001; 15, pp 255–294.
22. Keszei, S.; Simandi, B.; Szekely, E.; Fogassy, E.; Sawinsky, J.; Kemeny, S. *Tetrahedron: Asymmetry* **1999**, *10*, 1275–1281.
23. Simandi, B.; Keszei, S.; Fogassy, E.; Sawinsky, J. *J. Org. Chem.* **1997**, *62*, 4390–4394.
24. Anderson, N. G. *Org. Process Res. Dev.* **2001**, *5*, 613–621.
25. Lingenfelter, D. S.; Helgeson, R. C.; Cram, D. J. *J. Org. Chem.* **1981**, *46*, 393–406.
26. Newcomb, M.; Toner, J. L.; Helgeson, R. C.; Cram, D. J. *J. Am. Chem. Soc.* **1979**, *101*, 4941–4947.
27. Peacock, S. C.; Domeier, L. A.; Gaeta, F. C. A.; Helgeson, R. C.; Timko, J. M.; Cram, D. J. *J. Am. Chem. Soc.* **1978**, *100*, 8190–8202.
28. Hallett, A. J.; Kwant, G. J.; de Vries, J. G. *Chem.—Eur. J.* **2009**, *15*, 2111–2120.
29. Steensma, M.; Kuipers, N. J. M.; de Haan, A. B.; Kwant, G. *Chirality* **2006**, *18*, 314–328.
30. Steensma, M.; Kuipers, N. J. M.; de Haan, A. B.; Kwant, G. *Chem. Eng. Process.* **2007**, *46*, 996–1005.
31. Dzygiel, P.; Reeve, T. B.; Piarulli, U.; Krupicka, M.; Tvaroska, I.; Gennari, C. *Eur. J. Org. Chem.* **2008**, *7*, 1253–1264.
32. Pickering, P. J.; Chaudhuri, J. B. *Chirality* **1999**, *11*, 241–248.
33. Reeve, T. B.; Cros, J. P.; Gennari, C.; Piarulli, U.; de Vries, J. G. *Angew. Chem., Int. Ed.* **2006**, *45*, 2449–2453.
34. Takeuchi, T.; Horikawa, R.; Tanimura, T. *Anal. Chem.* **1984**, *56*, 1152–1155.
35. Tsukube, H.; Shinoda, S.; Uenishi, J.; Kanatani, T.; Itoh, H.; Shiode, M.; Iwachido, T.; Yonemitsu, O. *Inorg. Chem.* **1998**, *37*, 1585–1591.
36. Verkuijl, B. J. V.; Minnaard, A. J.; de Vries, J. G.; Feringa, B. L. *J. Org. Chem.* **2009**, *74*, 6526–6533.
37. Abe, Y.; Shoji, T.; Kobayashi, M.; Qing, W.; Asai, N.; Nishizawa, H. *Chem. Pharm. Bull.* **1995**, *43*, 262–265.
38. Prelog, V.; Stojanac, Z.; Kovacevic, K. *Helv. Chim. Acta* **1982**, *65*, 377–384.
39. Tan, B.; Luo, G. S.; Qi, X.; Wang, J. D. *Sep. Purif. Technol.* **2006**, *49*, 186–191.
40. Tan, B.; Luo, G. S.; Wang, H. D. *Tetrahedron: Asymmetry* **2006**, *17*, 883–891.
41. Tan, B.; Luo, G. S.; Wang, J. D. *Sep. Purif. Technol.* **2007**, *53*, 330–336.
42. Viegas, R. M. C.; Afonso, C. A. M.; Crespo, J. G.; Coelhoso, I. M. *Sep. Purif. Technol.* **2007**, *53*, 224–234.
43. Dimitrova, P.; Bart, H. J. *Chem. Eng. Technol.* **2009**, *32*, 1527–1534.
44. Kellner, K. H.; Blasch, A.; Chmiel, H.; Lämmerhofer, M.; Lindner, W. *Chirality* **1997**, *9*, 268–273.
45. Lindner, W.; Lämmerhofer, M. and Maier, N.M. EP Patent 0,912,563, 1997.
46. Schuur, B.; Winkelman, J. G. M.; Heeres, H. J. *Ind. Eng. Chem. Res.* **2008**, *47*, 10027–10033.
47. Schuur, B.; Floure, J.; Hallett, A. J.; Winkelman, J. G. M.; de Vries, J. G.; Heeres, H. J. *Org. Process Res. Dev.* **2008**, *12*, 950–955.
48. Schuur, B.; Hallett, A. J.; Winkelman, J. G. M.; de Vries, J. G.; Heeres, H. J. *Org. Process Res. Dev.* **2009**, *13*, 911–914.
49. Galan, A.; Andreu, D.; Echavarren, A. M.; Prados, P.; de Mendoza, J. *J. Am. Chem. Soc.* **1992**, *114*, 1511–1512.
50. Naemura, K.; Matsunaga, K.; Fuji, J.; Ogasahara, K.; Nishikawa, Y.; Hirose, K.; Tobe, Y. *Anal. Sci.* **1998**, *14*, 175–182.
51. Naemura, K.; Nishioka, K.; Ogasahara, K.; Nishikawa, Y.; Hirose, K.; Tobe, Y. *Tetrahedron: Asymmetry* **1998**, *9*, 563–574.
52. Steensma, M.; Kuipers, N. J.; de Haan, A. B.; Kwant, G. *J. Chem. Technol. Biotechnol.* **2006**, *81*, 588–597.
53. Steensma, M.; Kuipers, N. J. M.; de Haan, A. B.; Kwant, G. *Chem. Eng. Sci.* **2007**, *62*, 1395–1407.
54. Verkuijl, B. J. V.; de Vries, J. G.; Feringa, B. L. *Chirality* **2010**, , doi:10.1002/chir.20834.
55. Koska, J.; Haynes, C. A. *Chem. Eng. Sci.* **2001**, *56*, 5853–5864.
56. Atkins, P. W. *Physical Chemistry*, 5th ed.; Oxford University: Oxford, 1994.
57. Hein, Fr.; Meier, F. *Z. Anorg. Allg. Chem.* **1970**, *376*, 296–302.